Optica Applicata, Vol. LII, No. 4, 2022
DOI: 10.37190/oa220410

Fully negative near-zero ultra-flat dispersion photonic crystal fibers in E+S+C+L band

Yucheng Mao[1], Yiwu Ma[1,*], Ying Huang[1], Hua Yang[1,2,**]

[1]College of Computer Science and Electronic Engineering, Hunan University, Changsha 410082, People's Republic of China

[2]State Key Laboratory of Integrated Optoelectronics, Institute of Semiconductors, Chinese Academy of Sciences, Beijing 100083, People's Republic of China

[*]Corresponding author: myw@hnu.edu.cn

[**]Corresponding author: huayang@hnu.edu.cn

We demonstrate a modified hexagonal three-layer air-hole photonic crystal fiber (PCF) which presents a good ability of dispersion management. The proposed PCF not only achieved an ultra-flattened all-negative dispersion characteristics of 0.15085 ps/(km·nm) fluctuation within the wavelength range of E+S+C+L wavelength band but also has been able to obtain other interesting features such as low confinement loss. Furthermore, the quadrilateral and octagonal structures are investigated to compare the superiority of different structures and analyze why we chose the hexagonal one.

Keywords: photonic crystal fiber, ultra-flattened dispersion, onfinement loss, dispersion management method, supercontinuum (SC) generation.

1. Introduction

Optical fiber has become an extremely important component for communication systems nowadays. The chromatic dispersion becomes the critical factor that affects communication quality because the transmission rate, the distance, and the bandwidth are increased to meet the requirement of the modern optical communication. Therefore, photonic crystal fibers (PCFs) have been proposed in 1995 [1]. Photonic crystal fiber has been widely studied and applied due to its structural specificity and design flexibility which makes it possible to regulate the dispersion properties. Particularly, PCF has an extremely wide range of applications in the design and manufacture of ultra-flattened dispersion fibers. Controlling the flatness of PCF dispersion over a wide range of wavelength bands is still an ongoing challenge until today.

In the past 20 years, numerous researchers have proposed a variety of PCFs to obtain ultra-flat dispersion properties [2–19]. In order to improve the dispersion flatness and broaden the dispersion flatness range, photonic crystal fibers are designed with increasing complexity. A W-type single-polarization single-mode (SPSM) PCF [8]

was studied by DUNKE LU *et al*. with the dispersion 0.82 ± 0.30 ps/(km·nm). JIANFEI LIAO *et al*. have presented two types of hybrid cladding PCFs with different air-holes diameters, pitches and air-holes arranged fashions which exhibit a dispersion variation of 0.931 and 1.533 ps/(km·nm), respectively [12]. In 2014, a special rotations inner air -hole rings around the fiber core method was presented for engineering ultra-flattened PCF by JIN HOU *et al*. [14]. Recently, EXIAN LIU *et al*. proposed a photonic quasi-crystal fiber (PQF) with an octagonal dual-cladding structure [18]. By optimizing three geometric degrees of freedom, the PQF presents a dispersion of 0.014 ± 0.293 ps/(km·nm). The properties of this structure in generating the supercontinuum (SC) spectrum in anomalous dispersion region as well as the three zero-dispersion wavelengths (ZDWs) have been studied by us before [20]. Although some fiber designs have achieved exceptionally flat dispersion, few of them seem to have kept the flat dispersion range all within the normal dispersion region [21]. As we all know, both the modulation instability (MI) and optical solitons exist only in the anomalous dispersion region, where there is a bad effect on producing flat, broadband SC spectra [22] due to the internal pulse Raman scattering effect and the third-order dispersion effect. Therefore, to obtain an SC spectrum with good flatness, it would be better to control the input pulse in the normal dispersion region.

Hence, in this paper, we proposed a special hexagonal three-ring air-hole PCF [23] based on silicon with the dispersion –0.34074 ± 0.15085 ps/(km·nm). To obtain the best results, we conducted a comparative analysis of quadrilateral, hexagonal and octagonal structures, respectively, and finally found that the hexagonal structure is more favorable for fiber fabrication and practical applications. The structure of this article is as follows. Section 1 is a background introduction related to photonic crystal fibers. In Section 2, the finalized structure of the photonic crystal fiber and its dispersion and confinement loss characteristics are demonstrated. Section 3 presents the analytical methods for the properties of PCFs and how we achieved the ultra-flattened low confinement loss PCFs by analytical tuning. Then, the deficiencies of the octagonal and quadrilateral structures relative to the hexagonal structure are exhibited in Section 4. Finally, Section 5 gives a summary of this work.

2. Schematic diagram and chromatic dispersion results

The proposed three-ring hexagonal PCF is shown in Fig. 1, the pitches between the layers are equal to Λ, the diameters of the main and additional air holes for each ring are independent variables, the main-hole diameters from inside to outside are d_1, d_2, and d_3, respectively, and the extra-hole diameters are r_1, r_3. Moreover, the base material is silicon. It is clear to see that there are six parameters in this PCF model called Λ, d_1, d_2, d_3, r_1, and r_3, respectively. By tuning these parameters we can achieve a wide range of high-precision dispersion control, thus realizing the ultra-flat characteristics of photonic crystal fibers.

Figure 2 shows the ultra-flattened dispersion curves generated by our proposed structure with the structural parameters: Λ = 2.52 μm, $d_1 = 0.3143\Lambda$, $d_2 = 0.7399 d_1$,

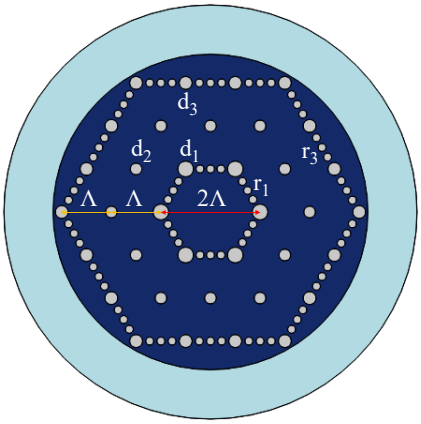

Fig. 1. Cross-sectional view of the structure of the photonic crystal fiber used in this paper.

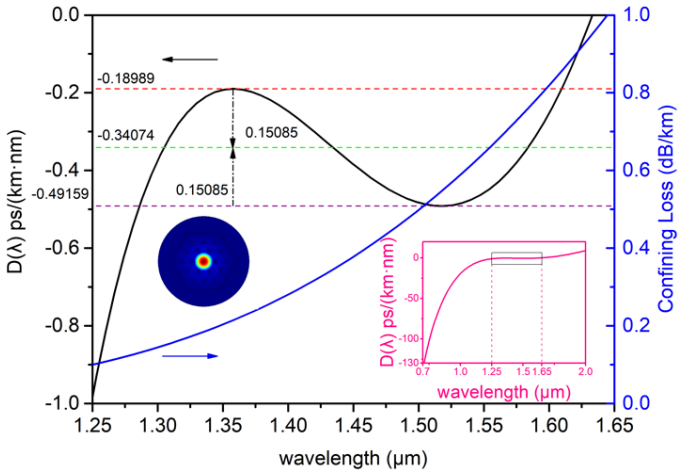

Fig. 2. Chromatic dispersion, confinement loss and mode diagram of the designed ultra-flattened PCF.

$d_3 = 0.82\,d_1$, $r_1 = 0.1136\,d_1$, $r_3 = 0.2336\,d_1$. The dispersion variation is within -0.34074 ± 0.15085 ps/(km·nm) over the E+S+C+L band and the confinement loss is less than 1 dB/km before 1.65 μm.

Apparently, by modifying the structural parameters, this structure of PCF can precisely control the dispersion, including dispersion flatness, flat-dispersion width, and dispersion amplitude magnitude. In this paper, we only discuss the control of dispersion flatness.

3. Dispersion engineering and analysis methods

In this section, we will describe how to implement a near-zero ultra-flattened PCF through dispersion management of this topology. As we mentioned before, there are

six parameters in this PCF to modulate dispersion. In order to achieve near-zero ultra -flattened characteristics in an ultra-wide band by adjusting the proposed PCF structure parameters, a comprehensive study was conducted considering the effects of six parameters on dispersion as well as confinement losses

For the purpose of accurate analysis of the characteristics of light propagation modes in this PCF, the full vector finite element method (FEM) combined with the perfectly matched layer (PML) is utilized in COMSOL Multiphysics 5.4. The eigenvalue problem derived from Maxwell's equations can be solved by FEM to obtain the modal effective refractive index. Then, the dispersion, confinement loss, effective mode field area, nonlinear coefficient and a series of parameters all can be obtained by using suitable equations.

Considering the single-mode operation in the PCF is in a dominant position, the multi-mode dispersion can be ignored. Hence, total dispersion is the superposition of waveguide dispersion D_{w} and material dispersion D_{m}. The chromatic dispersion can be obtained by the following expression:

$$D(\lambda) = -\frac{\lambda}{c}\frac{\mathrm{d}^2 \mathrm{Re}[n_{\mathrm{eff}}]}{\mathrm{d}\lambda^2} \tag{1}$$

where λ is the wavelength and c is the velocity of light in vacuum. The confinement loss can be obtained from the imaginary part of the effective refractive index as follows:

$$L_{\mathrm{c}} = 8.686 \times \mathrm{Im}[k_0 n_{\mathrm{eff}}] \tag{2}$$

where $k_0 = 2\pi/\lambda$ is the wave number in vacuum. The effective area of this PCF can be expressed as

$$A_{\mathrm{eff}} = \frac{\left(\iint |E|^2 \mathrm{d}x\mathrm{d}y\right)^2}{\iint |E|^4 \mathrm{d}x\mathrm{d}y} \tag{3}$$

where E is the electric field amplitude.

The nonlinear coefficient is defined by:

$$\gamma = \frac{2\pi}{\lambda}\frac{n_2}{A_{\mathrm{eff}}} \tag{4}$$

where λ is the wavelength in free space and $n_2 = 2.6 \times 10^{-20}$ m^2/W is the nonlinear refractive index of pure silica which represents the degree of nonlinear effects. In this paper, we focus on the analysis of the dispersion and the confinement loss characteristics.

In the first step, the approximate base parameters were first determined by a pre-experimental study, and on this basis the parameters were analyzed and optimized. For

better presentation of the results, we directly use the final parameters as the base parameters here.

Figure 3 shows the effect of six parameters on dispersion, including waveguide dispersion, material dispersion (black dash dot) and total dispersion(insets). Each parameter fluctuates up and down by 20% in the case of the base parameter. According to the results illustrated in Fig. 3, it is obvious that different parameters have different degrees of influence on the dispersion curves. The degree of influence on the dispersion curve is ranked from largest to smallest as Λ, d_2, d_1, r_1, d_3, and r_3.

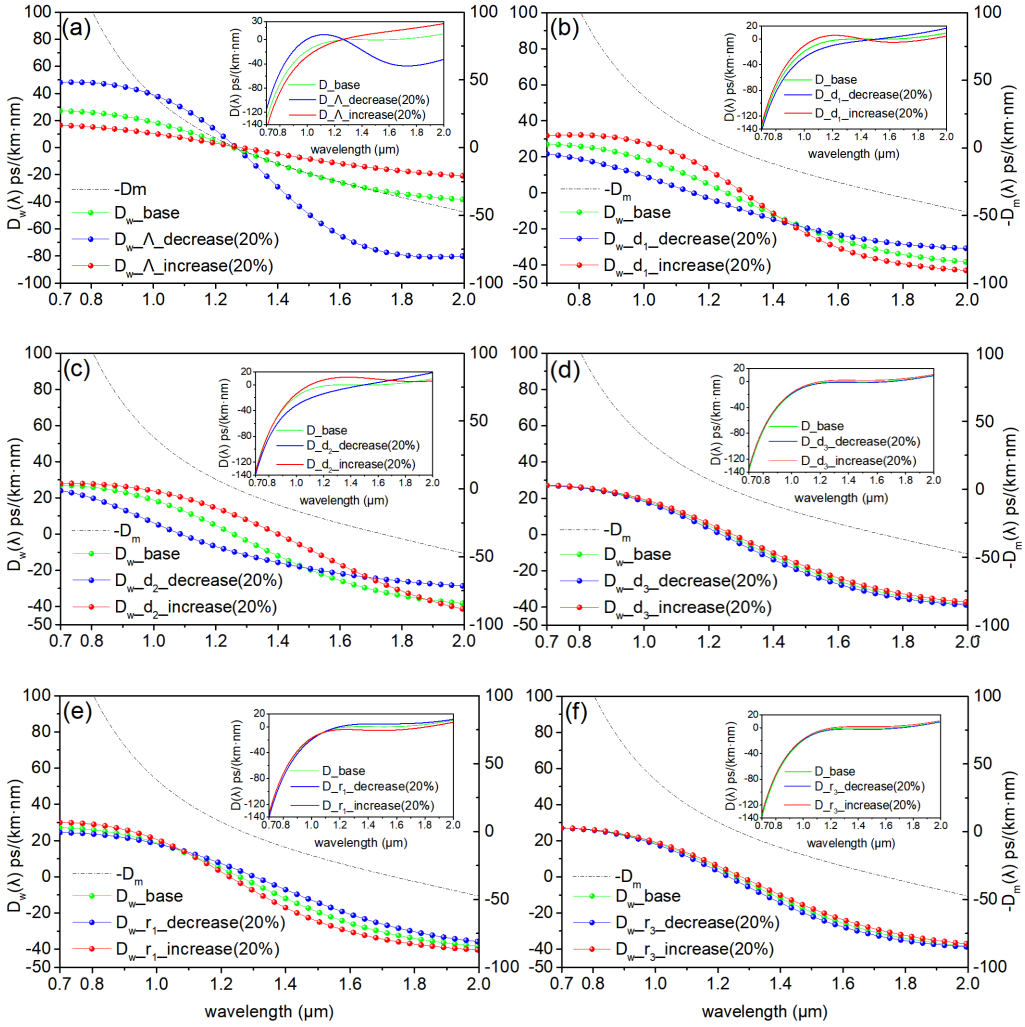

Fig. 3. Response graph of waveguide dispersion (main image), material dispersion (black dash dot), and total dispersion (inset) curves with parameter variation. (a) 20% fluctuation in Λ, (b) 20% fluctuation in d_1, (c) 20% fluctuation in d_2, (d) 20% fluctuation in d_3, (e) 20% fluctuation in r_1, and (f) 20% fluctuation in r_3.

From Fig. 3(a), when the pitch varied by 20%, the waveguide dispersion curve has a large shift. Specifically, the dispersion change is inversely proportional to Λ at short wavelengths and positively proportional at long wavelengths. Within this range of variation, the dispersion curve seems to rotate around a certain fixed wavelength point, which is approximately at the wavelength of 1.26 μm, in other words, the dispersion at this wavelength does not change. The same happens for d_1 and r_1 as shown in Fig. 3(b) and (e), while the difference is that the rotation point has changed and the proportionality between the dispersion and the parameters has been reversed before and after the rotation point. Figure 3(c) has demonstrated the impact of d_2 on disper-

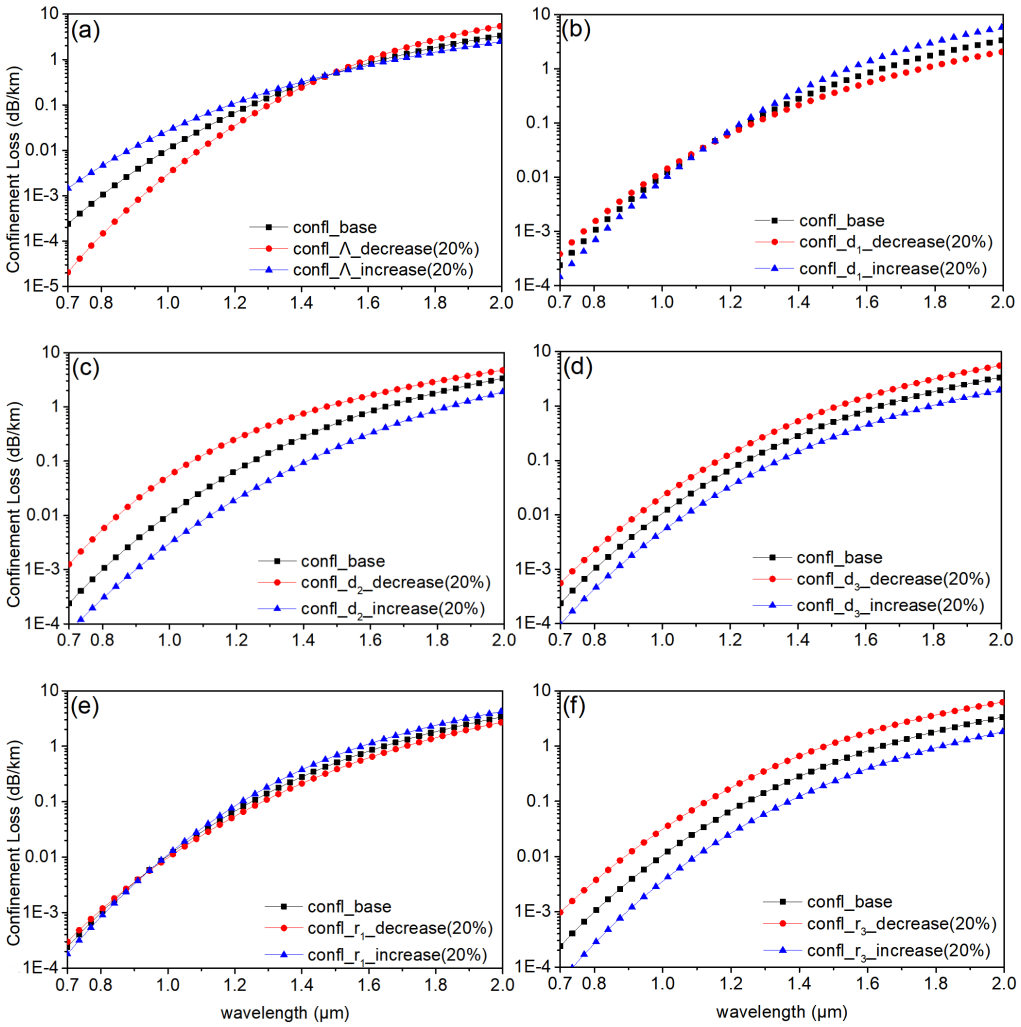

Fig. 4. Plot of the variation of the confinement loss curve with the change of PCF parameters. (a) 20% fluctuation in Λ, (b) 20% fluctuation in d_1, (c) 20% fluctuation in d_2, (d) 20% fluctuation in d_3, (e) 20% fluctuation in r_1, and (f) 20% fluctuation in r_3.

sion. Interestingly, the dispersion curve produces two rotation points within this range of variation, with rotation points of approximately 1.47 and 1.87 μm for decreasing d_2 and increasing d_2, respectively. As shown in Fig. 3(d) and (f), both d_3 and r_3 seem to have a small effect on the dispersion curves, and the dispersion values are proportional to the parameters over the entire range of the plotted bands.

In short, the effect of Λ on the dispersion curve is the greatest, as a change in pitch drives the expansion or contraction of the entire PCF structure. The influence of d_1 and d_2 on the dispersion curve is also significant while r_1 has a smaller impact on dispersion curve which can be explained by the fact that d_1 and d_2 have larger apertures relative to r_1. Since d_3 and r_3 are far away from the fiber core, they have less influence on the dispersion curve.

Confinement loss is also an important factor that must be considered during actual transmission. Although repeaters can play a good role in compensation, it would be more beneficial to make the fiber itself have excellent low confinement loss characteristics. Figure 4 shows the response curves of the confinement loss with different parameter fluctuations.

As shown in Fig. 4(a), the Λ has a strong effect on dispersion at short wavelengths, the degree of influence decreases with the wavelength increase until 1.5 μm, and slowly starting to increase again after 1.5 μm. Figure 4(b) and (e) demonstrate that the changes in d_1 and r_1 both have a relatively small effect on confinement loss and the long wavelengths are slightly more affected than the short wavelengths. The confinement loss curve always rotates around a specific wavelength when the three parameters Λ, d_1, and d_2 fluctuate up and down by 20%, *i.e.*, at this specific wavelength, the confinement loss does not change with the change of the parameters. However, a different situation occurs for the other three parameters as Fig. 4(c), (d) and (f) exhibit. In the whole plotted band interval, the confinement losses are always inversely proportional to the parameters size, the larger the parameters the smaller the confinement losses at the same wavelength. Through the previous dispersion analysis, we know that both d_1 and r_1 variations have a small effect on the dispersion curves, but the effect of these two parameters on the confinement loss is relatively large. Therefore, d_3 and r_3 can regulate the confinement loss characteristics well while maintaining the dispersion curve essentially unchanged.

4. Comparison of the superiority of quadrilateral, hexagonal and octagonal structures

The effect of each parameter on the dispersion curves and confinement losses has been learned and a series of ultra-flattened PCFs have been obtained by modifying the structure of conventional hexagonal air-hole PCF and adjusting the parameters, as described in the previous section.

So what would be the impact if we applied this approach to other types of photonic crystal fibers, such as quadrilateral structures, octagonal structures? Is it possible that

other structures will give better results than hexagonal structures? The answers to all these questions will be revealed by the following analysis.

The structure diagram, mode diagram and its height expression of the new PCF are shown in Fig. 5(a)–(c). The quadrilateral ones are shown in Fig. 5(g)–(i). For better comparison, graphs of the hexagonal structure are given in Fig. 5(d)–(f). All these fibers have the same structural parameters as a way to ensure the validity of the comparison experiment.

As can be seen from Fig. 5(b) and (e), the octagonal structure has better binding capacity and the energy is more concentrated at the fiber core which means that the octagonal structure transmits the optical signal more efficiently than the hexagonal struc-

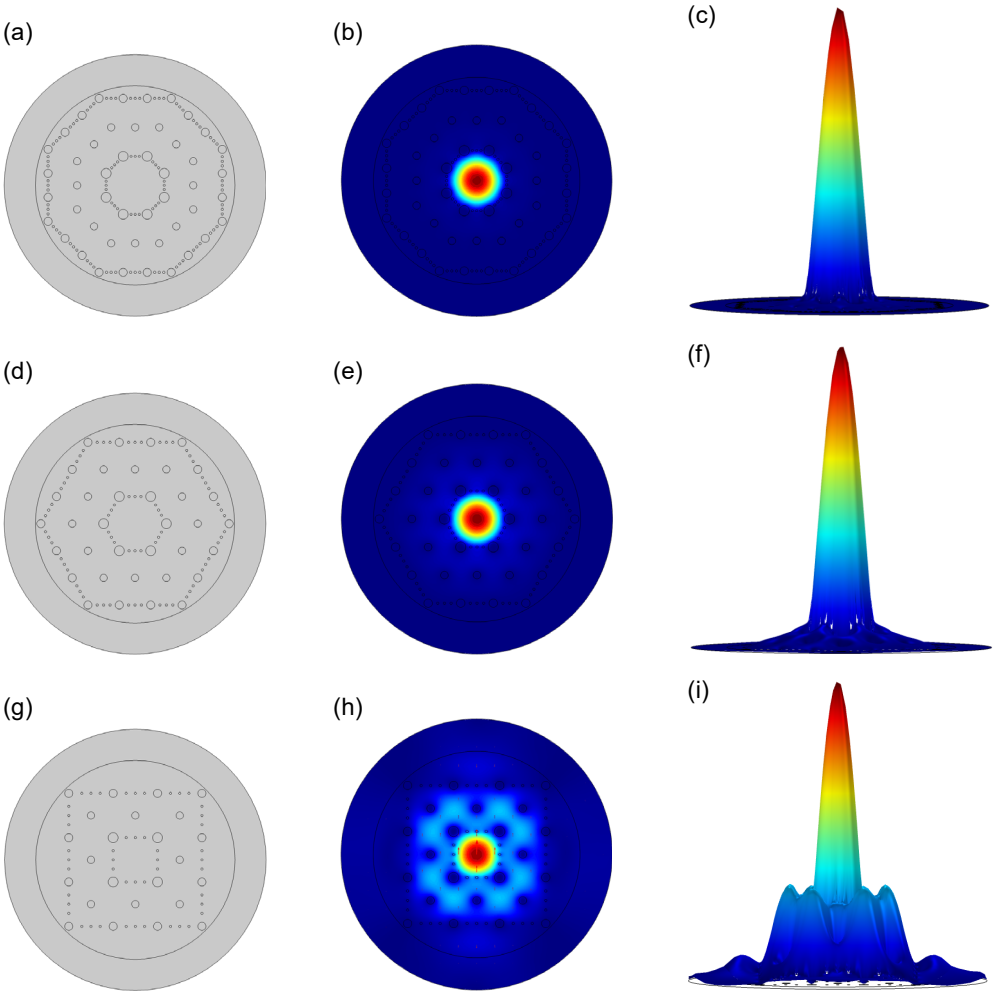

Fig. 5. Comparison of octagonal structure (a–c), hexagonal structure (d–f) and quadrilateral structure (g–i) PCF with the same structural parameters. (a, d, g) Structure diagram, (b, e, h) base mode pattern diagram, and (c, f, i) base mode height expression.

ture. This is also apparent from Fig. 5(c) and (f). The octagonal structure produces an abrupt change in energy distribution from the cladding to the core, while the hexagonal structure is gradual. In another word, the confinement loss of octagonal structure is less than the hexagonal one at the same wavelength.

Comparing the result shown in Fig. 5(e) and (h), it is clear that the mode field energy distribution of quadrilateral structure is not concentrated in the core region, and even higher order modes with less energy appear in the cladding which indicates that this structure may not be suitable for single-mode transmission and the confinement loss may be larger relative to hexagonal structure.

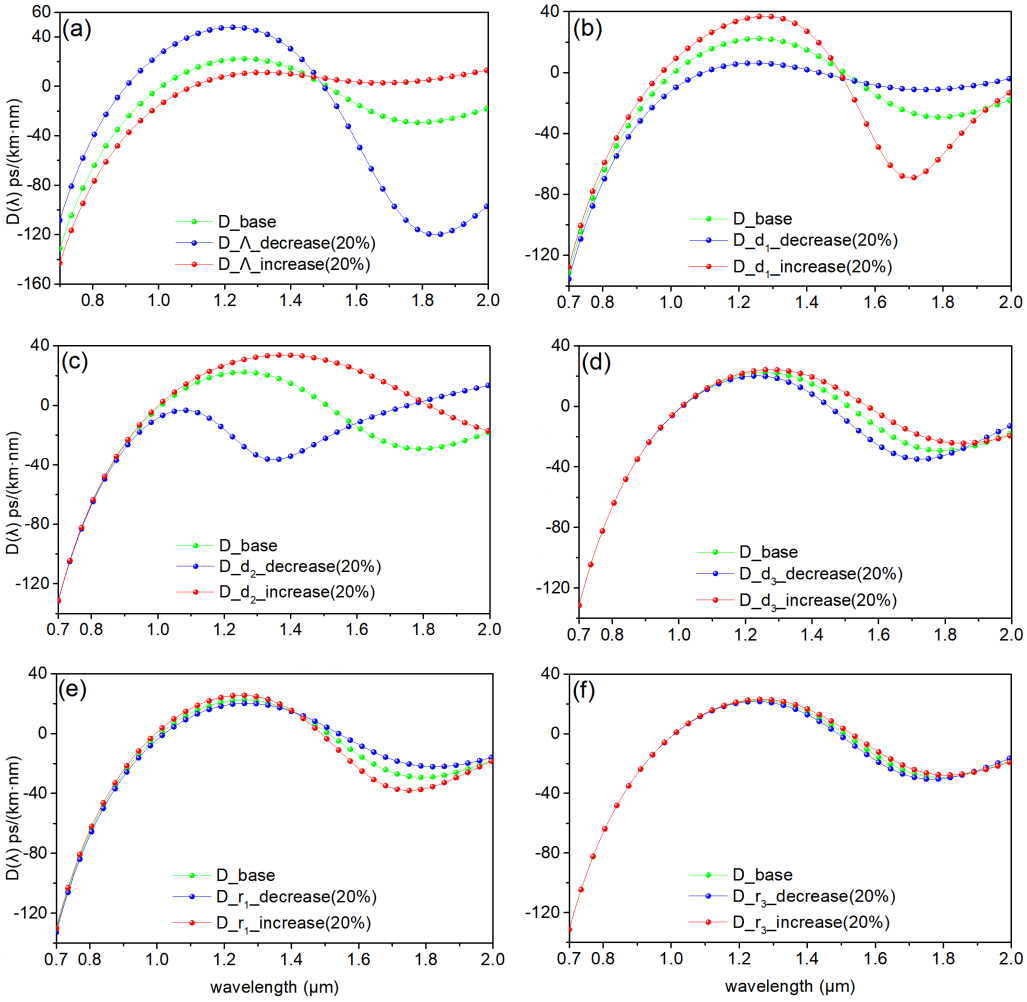

Fig. 6. Variation curves of octagonal PCF dispersion with fluctuation of fiber parameters. (a) 20% fluctuation in Λ, (b) 20% fluctuation in d_1, (c) 20% fluctuation in d_2, (d) 20% fluctuation in d_3, (e) 20% fluctuation in r_1, and (f) 20% fluctuation in r_3.

From the above analysis, it seems that the octagonal structure is more advantageous than the hexagonal structure. But in reality, we need to consider more factors, such as the robustness of the fiber structure. Figure 6 shows the response of the dispersion curves for octagonal structures as the parameters are varied.

It is obvious from Fig. 6(a)–(c) that for the octagonal structure, the dispersion curves change significantly when the fiber parameters Λ, d_1 and d_2 are shifted by 20%. For the hexagonal structure, the dispersion curve fluctuations are relatively small as exhibited in Fig. 3 before. The results in Fig. 6(d)–(f) show that although the fluctuations of the other three parameters d_3, r_1 and r_3 have relatively small effects on the dispersion curves of the octagonal structure, their fluctuations are still larger compared to those of the hexagonal one. This means that for octagonal structures, changes in their parameters will have a large impact on the dispersion curve, however, in the fiber fabrication and signal transmission, the actual structure parameters of the fiber will inevitably deviate from the design parameters because they will be affected by external stresses. In order to avoid this force majeure effect, the fiber dispersion should be made as insensitive as possible to changes in the fiber structure parameters. Therefore, in the comparison of octagonal and hexagonal structure, we choose the hexagonal structure as the superior structure.

As for the quadrilateral structure, we know from the above analysis that it cannot transmit in fundamental mode, and its loss will be relatively large, which is demonstrated in Fig. 7, so it would have been disregarded. Hence, in the comparison of these three different structures, we choose the hexagonal structure as the optimal choice.

The Table presents a comparison of the results of this design with other designs. The results show that the advantages of this design are: first, the dispersion fluctuation is small; second, the dispersion is all in the normal dispersion region near zero in the given band, which is conducive to the generation of supercontinuum.

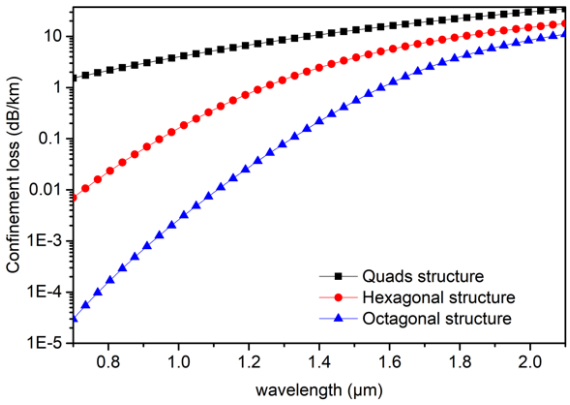

Fig. 7. Comparison of confinement loss curves of quadrilateral structure, hexagonal structure and octagonal structure with the same parameters.

T a b l e. Comparison for the results of the proposed PCF with the other studies.

Reference	Dispersion fluctuation [ps/nm·km]	Wavelength window [μm]	Wavelength range [nm]
[7]	1.00	1.100–1.600	500
[8]	0.30	1.120–1.510	390
[11]	1.00	1.262–1.722	460
[11]	1.50	1.218–1.750	532
[13]	0.1252	1.350–1.700	350
[18]	0.293	1.270–1.670	400
[19]	1.25	1.496–1.596	100
Proposed PCF	**0.15**	**1.280–1.610**	**330**

5. Conclusions

In a summary, a special three ring air-hole PCF is investigated in this work. In order to obtain the best results, the quadrilateral, hexagonal and octagonal structures were respectively analyzed and compared. The study results show that the hexagonal structure has superior performance. Based on this analysis, we take the hexagonal structure as the research object. By analyzing the effects of the size of Λ and the diameter of different air holes d_1, d_2, d_3, r_1, and r_3 on the dispersion curve, we know that some parameters have a greater effect on the dispersion and some have a smaller effect on the dispersion. Thus we first make a coarse adjustment for the parameters with a greater effect, and then make a fine adjustment for the parameters with a smaller effect when the dispersion curve is in the ideal range and finally we obtain the ultra-flattened dispersion characteristics (-0.34074 ± 0.15085 ps/(km·nm)) over the E+S+C+L wavelength band. The properties of this structured fiber may be illuminating for applications such as ultra-long-range transmission and SC generation. Further work will focus on the role of near-zero ultra-flat dispersion fiber in SC generation.

Acknowledgements
This work was supported by the National Key Research and Development Program of China (2018YFB0704000).

References

[1] Russell P.St.J., Birks T.A., Lloyd-Lucas F.D., *Photonic Bloch waves and photonic band gaps*, [In] *Confined Electrons and Photons*, Burstein, E., Weisbuch, C. [Eds], NATO ASI Series, Vol. 340, Springer, Boston, MA, pp. 585–633, DOI: 10.1007/978-1-4615-1963-8_19.

[2] Ferrando A., Miret J.J., Silvestre-Mora E., Andres M.V., Andres P., Russell P.St.J., *Designing a photonic crystal fiber with flattened dispersion*, Proc. SPIE 3749, 18th Congress of the International Commission for Optics, (19 July 1999), pp. 65–66, DOI: 10.1117/12.354920.

[3] Ferrando A., Silvestre E., Miret J.J., Andrés P., *Nearly zero ultraflattened dispersion in photonic crystal fibers*, Optics Letters **25**(11), 2000, pp. 790–792, DOI: 10.1364/OL.25.000790.

[4] FERRANDO A., SILVESTRE E., ANDRÉS P., MIRET J.J., ANDRÉS M.V., *Designing the properties of dispersion-flattened photonic crystal fibers*, Optics Express **9**(13), 2001, pp. 687–697, DOI: 10.1364/OE.9.000687.

[5] JINGYUAN WANG, CHUN JIANG, WEISHENG HU, MINGYI GAO, *Modified design of photonic crystal fibers with flattened dispersion*, Optics & Laser Technology **38**(3), 2006, pp. 169–172, DOI: 10.1016/j.optlastec.2004.11.016.

[6] BEGUM F., NAMIHIRA Y., ABDUR RAZZAK S.M., KAIJAGE S., NGUYEN HOANG HAI, KINJO T., MIYAGI K., ZOU N., *Design and analysis of novel highly nonlinear photonic crystal fibers with ultra-flattened chromatic dispersion*, Optics Communications **282**(7), 2009, pp. 1416–1421, DOI: 10.1016/j.optcom.2008.12.005.

[7] SHOBUG M.A., SAYED R., IFTEKHARUL FERDOUS A.H.M., *Characterization of hexagonal photonic crystal fiber for zero flattened dispersion with lower confinement loss and residual dispersion compensation over 500 nm wavelength bandwidth*, IOSR Journal of Electrical and Electronics Engineering (IOSR-JEEE) **11**(4), 2016, pp. 19–24, DOI: 10.9790/1676-1104041924.

[8] LU D., LI X., ZENG G., LIU J., *Dispersion engineering in single-polarization single-mode photonic crystal fibers for a nearly zero flattened profile*, IEEE Photonics Journal **9**(5), 2017, article no. 2700708, DOI: 10.1109/JPHOT.2017.2740951.

[9] HAXHA S., ADEMGIL H., *Novel design of photonic crystal fibres with low confinement losses, nearly zero ultra-flatted chromatic dispersion, negative chromatic dispersion and improved effective mode area*, Optics Communications **281**(2), 2008, pp. 278–286, DOI: 10.1016/j.optcom.2007.09.041.

[10] SHUQIN LOU, HONG FANG, HONGLEI LI, TIEYING GUO, LEI YAO, LIWEN WANG, WEIGUO CHEN, SHUISHENG JIAN, *Design of broadband nearly-zero flattened dispersion highly nonlinear photonic crystal fiber*, Chinese Optics Letters **6**(11), 2008, pp. 821–823, DOI: 10.3788/COL20080611.0821.

[11] JUI-MING HSU, *Tailoring of nearly zero flattened dispersion photonic crystal fibers*, Optics Communications **361**, 2016, pp. 104–109, DOI: 10.1016/j.optcom.2015.10.044.

[12] JIANFEI LIAO, JUNQIANG SUN, YI QIN, MINGDI DU, *Ultra-flattened chromatic dispersion and highly nonlinear photonic crystal fibers with ultralow confinement loss employing hybrid cladding*, Optical Fiber Technology **19**(5), 2013, pp. 468–475, DOI: 10.1016/j.yofte.2013.05.013.

[13] ANI A.B., FAISAL M., *Ultra-flattened broadband dispersion compensating photonic crystal fiber with ultra-low confinement loss*, [In] *2016 9th International Conference on Electrical and Computer Engineering* (*ICECE*), IEEE, 2016, pp. 243–246, DOI: 10.1109/ICECE.2016.7853901.

[14] JIN HOU, JIAJIA ZHAO, CHUNYONG YANG, ZHIYOU ZHONG, YIHUA GAO, SHAOPING CHEN, *Engineering ultra-flattened-dispersion photonic crystal fibers with uniform holes by rotations of inner rings*, Photonics Research **2**(2), 2014, pp. 59–63, DOI: 10.1364/PRJ.2.000059.

[15] PRANAW KUMAR, VIKASH KUMAR, JIBENDU SEKHAR ROY, *Design of quad core photonic crystal fibers with flattened zero dispersion*, AEU - International Journal of Electronics and Communications **98**, 2019, pp. 265–272, DOI: 10.1016/j.aeue.2018.11.014.

[16] MOHAMMADZADEHASL N., NOORI M., *Design of low-loss and near-zero ultraflattened dispersion PCF for broadband optical communication*, Photonics and Nanostructures - Fundamentals and Applications **35**, 2019, article no. 100703, DOI: 10.1016/j.photonics.2019.100703.

[17] MIN ZHANG, FANGDI ZHANG, ZHIGUO ZHANG, XUE CHEN, *Dispersion-ultra-flattened square-lattice photonic crystal fiber with small effective mode area and low confinement loss*, Optik **125**(5), 2014, pp. 1610–1614, DOI: 10.1016/j.ijleo.2013.10.003.

[18] EXIAN LIU, WEI TAN, BEI YAN, JIANLAN XIE, RUI GE, JIANJUN LIU, *Broadband ultra-flattened dispersion, ultra-low confinement loss and large effective mode area in an octagonal photonic quasi -crystal fiber*, Journal of the Optical Society of America A **35**(3), 2018, pp. 431–436, DOI: 10.1364/JOSAA.35.000431.

[19] XI LIU, LIHONG HAN, XIAOYU JIA, JINLONG WANG, FANGYONG YU, ZHONGYUAN YU, *Design of hybrid -core PCF with nearly-zero flattened dispersion and high nonlinearity*, Chinese Optics Letters **13**(1), 2015, article no. 010602, DOI: 10.3788/COL201513.010602.

[20] YING HUANG, HUA YANG, SAILI ZHAO, YUCHENG MAO, SHUYUAN CHEN, *Design of photonic crystal fibers with flat dispersion and three zero dispersion wavelengths for coherent supercontinuum generation in both normal and anomalous regions*, Results in Physics **23**, 2021, article no. 10403, DOI: 10.1016/j.rinp.2021.104033.

[21] LONG ZHENG, XIA ZHANG, XIAOMIN REN, HUIFANG MA, LEI SHI, YAMIAO WANG, YONGQING HUANG, *Dispersion flattened photonic crystal fiber with high nonlinearity for supercontinuum generation at 1.55 μm*, Chinese Optics Letters **9**(4), 2011, article no. 040601, DOI: 10.3788/COL201109.040601.

[22] JIFANG RONG, HUA YANG, YUZHE XIAO, *Accurately shaping supercontinuum spectrum via cascaded PCF*, Sensors **20**(9), 2020, article no. 2478, DOI: 10.3390/s20092478.

[23] YING HUANG, HUA YANG, YUCHENG MAO, *Design of linear photonic crystal fiber with all-positive/negative ultraflattened chromatic dispersion for the whole telecom band*, Optical Engineering **60**(7), 2021, article no. 076110, DOI: 10.1117/1.OE.60.7.076110.

Received December 21, 2021
in revised form March 2, 2022